

Apodization sensor performance for TOPAS fiber Bragg grating

Toto Saktioto¹, Khaikal Ramadhan², Yan Soerbakti³, Romi Fadli Syahputra⁴, Dedi Irawan⁵, Okfalisa⁶

^{1,2,3,4}Department of Physics, Math and Science Faculty, Universitas Riau, Pekanbaru, Indonesia

⁵Department of Education Physics, Educatin Faculty, Universitas Riau, Pekanbaru, Indonesia

⁶Department of Informatics Engineering, Universitas Islam Negeri Sultan Syarif Kasim, Pekanbaru, Indonesia

Article Info

Article history:

Received Mar 5, 2021

Revised Aug 31, 2021

Accepted Sep 11, 2021

Keywords:

Apodization
Fiber Bragg grating
Sensitivity
Sensor
TOPAS

ABSTRACT

Optical sensors have more capabilities than electronic sensors, and therefore provide extraordinary developments, including high sensitivity, non-susceptibility to electromagnetic wave disturbances, small size, and multiplexing. Furthermore, fiber Bragg grating (FBG) is an optical sensor with a periodically changing grating refractive index, susceptible to strain and temperature changes. As a sensor, FBG's performance required to optimize and improve the numerical apodization function and affect the effective refractive index is considered. The grating fiber's apodization function can narrow the full width half maximum (FWHM) and reduce the optical signal's side lobes. In all the apodization functions operated by FBG, Blackman has the highest sensitivity of 15.37143 pm/°C, followed by Hamming and Gaussian, with 13.71429 pm/°C and 13.70857 pm/°C, respectively, and Uniform grating fiber with the lowest sensitivity of 12.40571 pm/°C. Hamming, Uniform, and Blackman discovered the sensitivity for a strain to be 1.17, 1.16, and 1.167 pm/microstrain, respectively. The results obtained indicated that apodization could increase FBG's sensitivity to temperature and strain sensors. For instance, in terms of other parameters, FWHM width, Hamming had the narrowest value of 0.6 nm, followed by Blackman with 0.612 nm, while Uniform had the widest FWHM of 1.9546 nm.

This is an open access article under the [CC BY-SA](https://creativecommons.org/licenses/by-sa/4.0/) license.



Corresponding Author:

Toto Saktioto

Department of Physics, Math and Science Faculty

Universitas Riau

Kampus Bina Widya km 12.5 Simpang Baru Pekanbaru 28293, Indonesia

Email: saktioto@yahoo.com

1. INTRODUCTION

Fiber Bragg grating's (FBG) discovery has been an early milestone in optoelectronics' history, and these fundamental discoveries yielded the incredible application felt today. Nowadays, extensive applications have greatly expanded, for instance, optical communications, optical sensing, data filters, dispersion compensators, and monitoring of material health structures to applications in the medical world as biosensors. In optical communication, FBG is used as a dispersion compensator [1] to produce a long-range data transmission, with or without an amplifier. This is also applied in optical filters [2], [3], filtering the transmitted wavelengths due to periodic changes in the grating, as well as increasing and reducing in wavelength division multiplexing communication, a technology with the ability to combine several optical

signals onto one fiber, using various light and laser wavelengths, to allow bidirectional communication within a single fiber, in optical sensing or monitoring applications [4]–[6].

FBG sensor components are sensitive to physical quantities changes and have better performance conventional or electronic counterparts. Based on the application type, the sensor is built on a fiber core with the ability to detect changes in physical parameters, including strain [7], [8], temperature [9], [10], pressure [9], and other parameters. Furthermore, FBG is superior to mechanical or electronic sensors due to the coding of information measured in wavelengths, thus, reducing connector and power losses, working in nanoscale sensors, and being more sensitive to physical changes [11].

As an optical sensor, FBG has developed and become a topic widely used researched in the last two decades. Several developments in applicable research on FBG have been reported, including as a smart textile in real-time respiratory monitoring in humans [12], heart frequency monitoring [13], as well as temperature and pressure monitoring, hybridized with woven thermoplastic composite fabrics [14]. Also, numerical experiments in improving FBG sensor performances have been widely studied with cyclic olefin copolymer, or called tool for particle simulation (TOPAS) material, having a higher sensitivity than Tera flex and pure silica materials [15]. The results showed apodization was able to narrow the full-wave half maximum (FWHM) in FBG. According to the researcher [16], a π phase with several apodization functions, including Gaussian, sinus, nuttall, Blackman, and raised cosine, is recommended for high-temperature monitoring sensors in electric transformers. Meanwhile, [17] reported FBG with nuttall apodization has a high sensitivity in monitoring sea surface temperature, with hydrophobic polymer-coated FBG. Fiber optical sensor based temperature sensing methodology includes, interferometric sensors [18], [19], photonic crystal fiber sensors [20] and FBG [21], [22].

FBG is often seen as a component of an optical filtering segment along an optical fiber core describing a specific wavelength. Based on the grating's shape and structure, it is generally classified as homogeneous and apodized. Uniform FBG is inherently sensitive to external strain and temperature changes, and this sensing property is viewed as a wavelength shift in the sensing unit's spectrum of reflection. The presence of more side lobes characterizes the shown homogeneous FBG spectrum, and the energy is very close to the peak wavelength. These side lobes are produced as noise problems that should be filtered. Using apodization and FBG sensitivity modification, the optical problems can be solved. Thus, the sensor's detection accuracy is reduced [12], [13], [23].

Therefore, this research aims to design, simulate and analyze performance as a component of temperature and strain sensors to produce a sensitive one, to be optimized with Blackman, Hamming, and Gaussian apodizations, one of the techniques to reduce side lobes, and consequently, produce a narrow and sensitive signal. The parameters which are considered for the determination of the effect of sensitivity are the grid length and the variation of apodization with TOPAS material [15]. This method utilizes analysis by simulating the fiber sensor component in the numerical experiment, analyzing the Bragg wave peak shift for each change in temperature and strain, and subsequently optimizing the sensor's performance to be validated in the OptiSystem software.

2. THEORETICAL CONSIDERATION

Optical fiber is a light transmission medium with the ability to carry information in voice and video data. It was first introduced in the world of telecommunications by Charle Kao. In application, this technology will convert an electrical signal into an optical signal and back into an electrical signal at the receiver [24], [25]. Charle Kao also proposed light is transmitted through silica fibers with the ability to conduct light [26], [27], and after the discovery of optical fibers, many developments aside from silica have occurred, efficiently transmitting light, including germanium, TOPAS, Tera Flex, plastics, and polymers. Thus, optical fibers are suitable for replacing conventional counterparts functioning as power cables and have numerous advantages over conventional electronic cables, mainly because the data transmitted is modulated by laser or light and, therefore, dangerous. Another advantage is the rapid, accurate, and relatively stable transmission of data to environmental conditions, compared to conventional cables. Therefore, optical fibers are useful for transmitting data across continents with susceptibility to electromagnetic waves, resulting in no wave interference, resistance to high temperatures, small transmissive attenuation, and large bandwidth [28].

In addition, FBG can reflect specific wavelengths, called Bragg wavelengths, and transmit other wavelengths due to a grating in the fiber core. The grid has a periodic pattern, and light is scattered after hitting the grind, which is called the Bragg effect. Bragg wavelength λ_B depending on the grid period and FBG guiding properties, including the refractive index n_{eff} is formulated mathematically as shown in (1) [29], [30].

$$\lambda_B = 2n_{eff}\Lambda \quad (1)$$

Meanwhile, the formula for calculating the refractive index distribution, $n_{eff}(z)$ as long as FBG, is outlined (2).

$$n_{eff}(z) = n_0 + f(z)\Delta n_{ac}v \cos\left(\left(\frac{2\pi}{\Lambda}\right)z + \theta(z)\right) \quad (2)$$

Where z represents position, n_0 denotes the initial refractive index, Λ is grating period, Δn_{ac} denotes the refractive index modulation amplitude, $f(z)$ connotes the apodization function, and $\theta(z) = 2\pi Cz^2/\Lambda$ is a chirp function where, C is the chirp parameter, and v represents peripheral visibility.

In (1) and (2) proportionally relate to the grating variables for temperature (T), strain (L), and changes in wavelength ($\Delta\lambda$). By taking X mathematically, this relationship is expressed in (3).

$$\Delta\lambda_b = \frac{d\lambda_b}{dX}\Delta X = \lambda_b\left(\frac{\delta n_{eff}}{n_{eff}} + \alpha\right)\Delta X \quad (3)$$

Where $\delta n_{eff}/n_{eff}$ represents the sensitivity normalized from the modal refractive index and α denotes the coefficient of change in physical length, depending on parameter X .

FBG acts as a sensor in cases where changes in physical parameters can shift the Bragg's wavelength to the measured quantities, including temperature, strain, hydrostatic pressure, or refractive index from the function, as shown in (3) [31]. The Bragg wavelength's shift in measuring temperature and strain is influenced by the material's thermo-optic coefficient α and thermal expansion δ . One can measure temperature and pressure simultaneously as shown in (4).

$$\Delta\lambda_b = \lambda_b(\alpha + \delta)\Delta T = \lambda_b\left(\frac{1}{n_{eff}}\frac{\Delta n_{eff}}{\Delta T} + \frac{1}{\Lambda}\frac{\Delta\Lambda}{\Delta T}\right)\Delta T \quad (4)$$

Meanwhile, insensitivity to strain, the Bragg wavelength's shift is influenced by the optical strain coefficient, Poisson ratio, refractive index, and thermal expansion coefficient, as shown in the (5).

$$\Delta\lambda_b = \lambda_b(1 - \rho_e)\delta \quad (5)$$

Where ρ_e represents the optical strain coefficient defined as (6).

$$\rho_e = \frac{n^2}{2}(\rho_{12} - v(\rho_{11} + \rho_{12})) \quad (6)$$

And ρ_e connotes the Poisson's ratio while ρ_{11} and ρ_{12} denoting tensors strain.

Naturally, the FBG sensor is hard to measure one temperature parameter or strain only, both quantities are measured simultaneously, as shown by (7).

$$\Delta\lambda = k_t\Delta T + k_e\Delta\delta + \Delta k_t\Delta k_e\Delta\delta \quad (7)$$

FBG's performance is possibly increased by apodization, a technique where unfavorable parameters are removed from the reflected light spectrum. However, there are some disadvantages, including the reduced amplitude of the spectrum's reflectivity peak. Several applications apply different apodization, including filtering, dispersion compensation, wavelength adjustment, and sensing in optical and optoelectronic communications, as well as improved performance in temperature and range sensors [14]. According to previous research results, the best profile apodization in FBG's account as a temperature and strain sensor was the Gaussian function, with a sensitivity of 14 pm/°C and 0.81 $\mu\text{m}/\text{microstrain}$ [15].

Several profiling types and the respective functions are outlined below [28]:

– Uniform

$$A(x) = 1, \text{ where } 0 \leq x \leq L \quad (8)$$

– Gaussian function

$$A(x) = \exp\left(-\ln 2 \left(\frac{2\left(x-\frac{L}{2}\right)}{0.5L}\right)^2\right), \text{ where } 0 \leq x \leq L \quad (9)$$

– Hamming (Happ-Genzel) function

$$A(x) = 0.54 - 0.46 \cos\left(\frac{2\pi x}{L}\right), \text{ where } 0 \leq x \leq L \quad (10)$$

– Nuttall-Blackman function

$$A(x) = 0.3635819 - 0.48917755 \cos\left(\frac{2\pi x}{L}\right) + 0.1365996 \cos\left(\frac{4\pi x}{L}\right), \text{ where } 0 \leq x \leq L \quad (11)$$

– Tanh function

$$A(x) = \tanh\left(4\frac{x}{L}\right) \tanh\left(\frac{1-x}{L}\right), \text{ where } 0 \leq x \leq L \quad (12)$$

Apodization is a technique to increase the Bragg grating fiber's sensitivity. Numerous studies have been reported on the effect of modifying apodization [32], [33], including the Nuttall-Blackman function's apodization to suppress the reflection spectrum's lobe side, compared to no apodization or Uniform type. The lobe's narrower side gives the FBG sensor a high sensitivity. A study by the researcher [15] in monitoring the electric transformer's high temperature, using Bragg grating fiber with phase π , showed FBG was superior to Sinusoidal type for each apodization. In this study, the temperature and strain FBG sensors' performance is to be optimized with variations in apodization, grating length, and reflection peak for respiratory monitoring applications in humans.

3. RESEARCH METHODOLOGY

This research use TOPAS material. The TOPAS (cycoelefin copolymer) [34] material FBG component is designed with parameters (thermo-optic coefficient is $-9.3 \times 10^{-5} \text{ } ^\circ\text{C}^{-1}$ and thermal expansion is $6 \times 10^{-5} \text{ } ^\circ\text{C}^{-1}$) and quantities affecting the Bragg grating fiber's performance. Furthermore, the simulation results provide an overview of changes in the Bragg wavelength to the varied parameters (10 to 50 mm grating length), and the data obtained from FWHM is to be analyzed to produce a more suitable sensor. Figure 1 shows the simulation operated on the OptiSystem software. Subsequently, the spectrum profile is obtained, and the changes in the reflection wave peaks concerning temperature and strain are depicted.

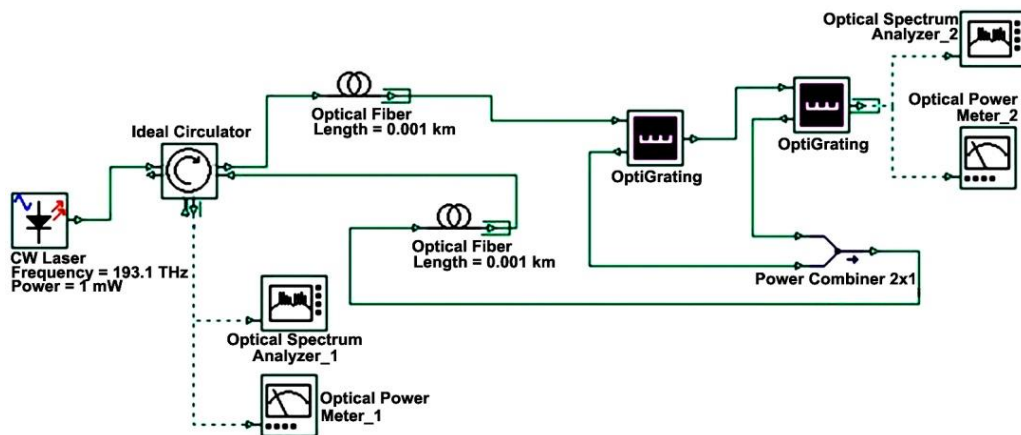


Figure 1. FBG sequences on OptiSystem

FBG is designed based on the core's geometry and refractive index of the core, cladding, and grating shape, according to the parameters of the TOPAS material, with a core refractive index of 1.53 and a cladding refractive index of 1.525 [34], [35], earlier defined (dialog box: side lobe left's (SLL), side lobe right's (SLR), peak) as parametric components. After passing the grating, the light source's wavelength is filtered [2].

The proposed system transmitter comprises a laser with power and frequency of 1 mW and 193.1 THz, respectively, connected to a circulator with a 1549 nm center wavelength. Subsequently, the circulator makes a signal loop with a 10 m initial optical fiber length, related to the first FBG data input design as a temperature sensor parameter and the second as a strain sensor. The FBG design's second reflection signal is then collected on the 2×1 power combiner and connected again to the circulator with 10 m optical fiber. In addition, the output signal on the circulator is monitored by an optical spectrum analyzer and optical power meter (OPM) to measure the signal shift.

4. RESULTS AND ANALYSIS

In this study, the effect of apodization was numerically investigated to determine FBG's impact on changes in temperature and strain. The apodization design used was Gaussian, Tanh, Hamming, and Blackman function, with a core refractive index and sleeve of 1.53 and 1.525, respectively, at a center wavelength of 1549 nm well as a modulation index parameter of 4×10^{-4} , and a 50 mm grating length.

4.1. Changes in the peak wavelength of Bragg with temperature

The Bragg wavelength is the wavelength of reflection, and after passing through the grid, part of the light is continued, while the remaining is reflected. In this simulation, the thermo optical coefficient is equal to the thermal expansion coefficient according to the TOPAS material. Figure 2 shows the change in Bragg wavelength peak over temperature.

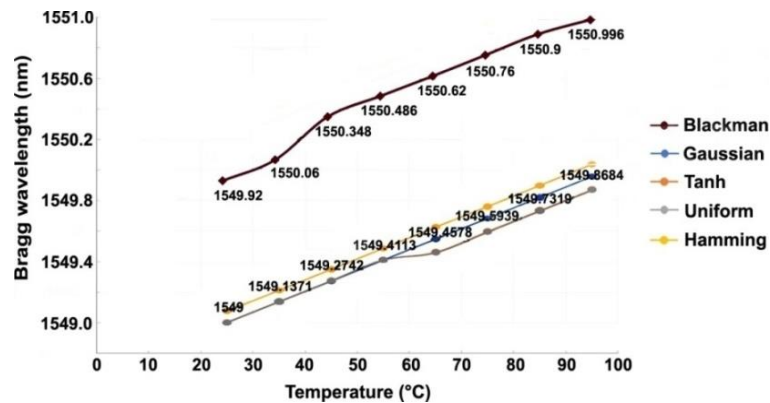


Figure 2. The shift of the Bragg wave crest to temperature

The Hamming and Gaussian apodization functions are almost linear, and so is the change in peak wavelength concerning temperature. At 25 °C, Gaussian, Tanh, and Uniform apodizations produce a peak wavelength of 1549 nm, while Hamming gives 1549.077 nm, with a 0.077 nm increase, and the average results are almost the same. Furthermore, the temperature change is 10 °C, the center wavelength is 1549 nm, and most of the Bragg wavelength peaks for each function have different FWHM widths. This, in turn, affects the peaks produced by each temperature change. The Bragg wavelength peak's linearity over temperature changes for Blackman apodization is small compared to other apodization functions. However, Blackman has higher sensitivity compared to other apodization functions.

Table 1 shows the sensitivity of each apodization function. Generally, the Bragg wavelength's phase shift is influenced by the useful refractive index n_{eff} , as shown in (2), meaning the apodization function and chirp function influence the Bragg grating fiber sensor's effective refractive index. This takes a linear chirp function and taper of 0.05 and 0.5, respectively. FBG with an apodization function has higher sensitivity than Uniform one without an apodization function, as shown in (2). The highest Bragg wave's peak shift of 15.37143 pm/°C was obtained with the Blackman apodization function, followed by Hamming and Gaussian, with 13.71429-13.70857 pm/°C, respectively, while the lowest sensitivity of 12.40571 pm/°C was obtained in the Uniform apodization, at a temperature range of 25 °C (room temperature), to 95 °C, in increments of 10 °C. This result is more significant compared to previous reports [12]. In addition, the sensor one with the highest sensitivity value of 14 pm/°C is Gaussian [13]. In monitoring high-temperature changes in wave crests, FBG sensors exhibited a sensitivity of 14.26 pm/°C, at a temperature range of -50 °C to 250 °C, and a 10 mm diameter of modulation refractive index, as well as grating length. In this study, the Blackman apodization function showed the best performance.

Table 1. Sensitivity of each apodization to temperature

Apodization	Sensitivity (pm/°C)
Gaussian	13.70857
Tanh	12.46429
Uniform	12.40571
Hamming	13.71429
Blackman	15.37143

4.2. Change in wavelength of Bragg with strain

The Bragg wave peak's shift to strain is more linear, and the sensor's measurement was apodized to strain, using the photoelastic coefficient $\rho_{11}=0.121$, $\rho_{12}=0.27$ with a 0.17 Poisson ratio, in the range of 100 microstrain to 200 microstrain [30]. Blackman and Hamming apodization functions can increase the strain sensor's sensitivity, compared to the Uniform counterpart of 1.17, 1.16, and 1.167 pm/microstrain, respectively. This result is higher, compared to previous reports, with a sensitivity of 0.84 microstrain [12].

4.3. Transmission and reflection of light for each FBG apodization

Figure 3 (a) shows the identification of reflection and transmission wavelengths, with a central material having a wavelength of 1549 nm and a 50 mm grating length. According to the Figure 3 (a), Hamming side lobes are in a low wavelength range of 1550-1550.6 nm, and the difference between the side and main lobes. Figure 3 (b) shows Blackman main lobe has a more excellent value compared to Hamming. However, this slight difference between the side and main lobes indicates a poor performance in temperature and strain measurements, where the wavelength is shown in the range 1549.4-1550.6 nm. According to Figure 3 (c), the Uniform profile has the smallest side lobe, ranging between 0 dB to -40 dB, followed by Blackman and Hamming, ranging between 0 dB to -80 dB and 0 dB to -60 dB, respectively. This difference between the primary and side lobes indicates poor performance in Uniform apodization. Figure 3 (d) shows the Gaussian profile, the main lobe in the -80 dB range, as well as larger main and side lobes, compared to the Uniform counterpart. Figure 3 (e) shows the transmission and reflection wavelengths range of 1548.5-1549.5 nm, indicating poor performance in strain and temperature monitoring, describing Tanh apodization and the range of 0 dB to -80 dB, with the Bragg wavelength at a value of -20 dB.

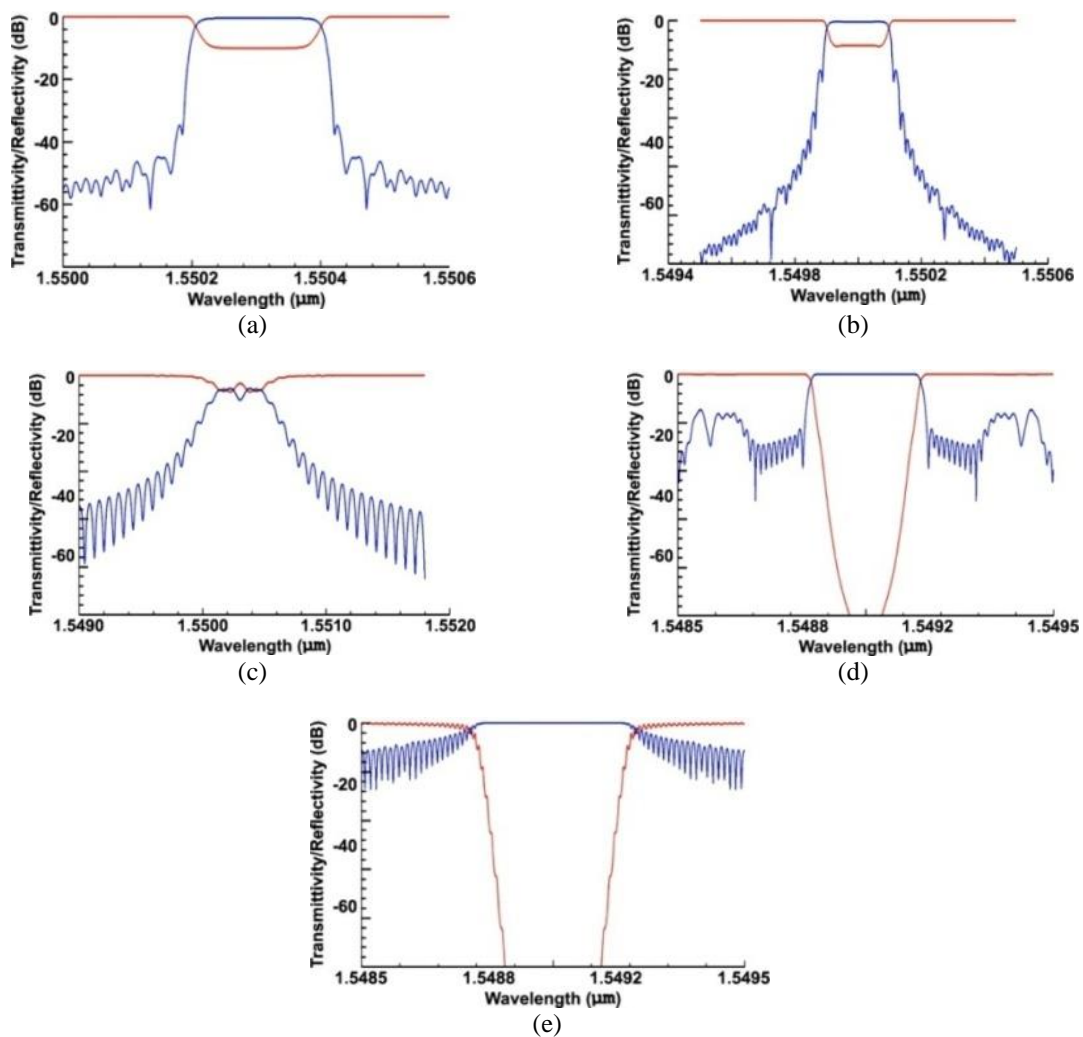


Figure 3. FBG spectrum for each apodization function: (a) Hamming, (b) Blackman, (c) Uniform, (d) Gaussian, and (e) Tanh

4.4. FWHM side lobe and ripple factor values

Blackman apodization for the wavelength range of 1550-1552 nm shows the side lobe left's (SLL) value and position is not found and the side lobe right's (SLR) value, place, and ripple factor. A low sidelobe value provides a good FBG sensor performance [28]. The following are some of the specific parameters obtained from each type of apodization for the FBG sensor as shown in Table 2.

Shown from Table 2 the width of each FWHM apodization, with the best FBG sensor performance for FWHM parameters are Hamming, Blackman, and Gaussian apodization with a width of 0.6 nm, 0.612 nm, and 0.636 nm respectively, the narrower the FWHM will give sensitive results. Monitoring temperature and strain by the lattice fiber sensor compared to the Uniform apodization value. Hamming, Blackman, and Gaussian apodization are also able to improve the performance of the Bragg grid sensor so that the output signal from FBG can be narrowed, if seen from the ripple factor value, Uniform FBG has the most value high and indicates a good performance, namely -0.99999, followed by Tanh apodization -0.99998 and Gaussian apodization -0.99836. In this case, the Blackman apodization did not reveal the value of the ripple factor to the left lobe and the right side lobe, this occurred in the wavelength range of 1550-1552 nm. Blackman apodization formed a small Bragg wavelength response. The difference between the main lobe and the left side of the Blackman apodization indicated a good performance, this happened because it had the largest main and left lobe size, which was 0.566 nm followed by Tanh and Uniform, while Gaussian apodization had a small main and side lobe difference, namely 0.372 nm. For the right side lobe, the Hamming apodization also had a bigger difference of 0.754 nm.

Table 2. FBG sensor analysis for each apodization with a grating length of 10 mm and a temperature of 25 °C

Parameter	Unit	Uniform	Gaussian	Tanh	Hamming	Blackman
Bandwidth	nm	1.9546	0.636	1.95	0.6	0.612
Peak position	nm	1550.88	1550.88	1550.88	1550.786	1550.8
Peak value	dB	-0.00026	-0.05325	-0.00033	-40.9078	-36.2341
SLL position	nm	1550.426	1550.508	1550.426	1550.22	-
SLL value	dB	-9.78892	-32.8936	-10.3135	-62.4393	-
SLR position	nm	1551.335	1551.254	1551.334	1551.54	-
SLR value	dB	-9.79369	-32.8994	-10.3156	-62.4467	-
Ripple factor	-	-0.99999	-0.99836	-0.99998	-0.24552	-

4.5. Results from OptiSystem

The OptiSystem simulation input the FBG design for each apodization at the same temperature, and the power of lightwave reflection and transmission and the form of graph response was obtained. Table 3 shows the power produced after running the optical circuit (Figure 1). Based on each OPM output power result, column 1 shows OPM's power after the signal passes through FBG. Blackman apodization was discovered to have the greatest continuous power of 999.952 μW , followed by Hamming and Gaussian, with 999.95 μW and 999.81 μW , respectively. The sensitivity results also show these three apodizations have high sensitivity. Thus, more power is transmitted after OPM detection, where the initial laser signal inputted in the optical circuit is 1 mW.

Subsequently, the signal is forwarded to the FBG 2 component, similar to the optical circuit above (Figure 1), partially delivered and reflected, and the two signals produced are collected on the 2x1 power combiner for further detection of the output power. In this second OPM, Uniform apodization's output power of 19.076 μW is significantly greater, compared to the others, followed by Tanhapodization with 17.16 μW , while Blackman has the smallest output power of $556.95 \times 10^{-6} \mu\text{W}$.

Table 3. Apodization forms of power

Apodization	Power Transmissions (μW)	Power Reflections (μW)
Uniform	952.077	19.076
Tanh	957.925	17.16
Hamming	999.95	0.002925
Gaussian	999.81	0.079213
Blackman	999.952	556.95×10^{-6}

5. CONCLUSION

The TOPAS FBG sensor with Blackman apodization has the most extraordinary sensitivity of 15.37143 $\text{pm}/^\circ\text{C}$ compared to other apodized grating fiber sensors. In contrast, the Bragg TOPAS grating fiber sensor in measuring Uniform apodization strain has the highest sensitivity of 1.167 $\text{pm}/\text{microstrain}$. Generally, Gaussian apodized FWHM has a better performance with a width of 0.36045 nm, while the

Blackman has the widest FWHM of 0.552 nm. In addition, Hamming has the highest difference between the left side and the main lobes compared to the others. This apodization does not show the side lobe values and the position of graph transmission as well as reflection signal, and between 1550-1552 nm, a small output signal is obtained. Thus, there are no ripples and side lobes. The apodization right side lobe also indicates the best performance as a bigger difference of 0.754 nm was obtained in the optical circuit. Also, the apodization with high sensitivity has reflection power.

ACKNOWLEDGEMENTS

The authors are grateful to the Universitas Riau, Pekanbaru Indonesia, through the Institute for Research and Community Service, to provide academic support in facilitating this research during 2021.

REFERENCES

- [1] S. A. Tahhan, M. H. Ali and A. K. Abass, "Characteristics of Dispersion Compensation for 32 Channels at 40 Gb/s under Different Techniques," *Journal of Optical Communications*, vol. 41, no. 1, pp. 57-65, Nov. 2019, doi: 10.1515/joc-2017-0121.
- [2] Saktioto *et al.*, "Birefringence and Polarization Mode Dispersion Phenomena of Commercial Optical Fiber in Telecommunication Networks," *Journal of Physics: Conference Series*, vol. 1655, no. 1, Oct. 2020.
- [3] I. Navruz and N. F. Guler, "A Novel Technique for Optical Dense Comb Filters using Sampled Fiber Bragg Gratings," *Optical Fiber Technology*, vol. 14, no. 2, pp. 114-118, Apr. 2008, doi: 10.1016/j.yofte.2007.09.004.
- [4] C. S. R. Gurusamy and Murthy, "WDM optical networks concepts, design, and algorithms," *New Jersey: Prentice Hall PTR*, 2002.
- [5] D. Irawan, T. Saktioto, and J. Ali, "Linear and triangle order of NX3 optical directional couplers: Variation coupling coefficient," *Proceedings of SPIE - The International Society for Optical Engineering*, Aug. 2010, doi: 10.1117/12.862573.
- [6] D. Irawan, T. Saktioto, and J. Ali, "An optimum design of fused silica directional fiber coupler," *Optics*, vol. 126, no. 6, pp. 640-644, Mar. 2015, doi: 10.1016/j.ijleo.2015.01.031.
- [7] B. A. Tahir, J. Ali, M. Fadhali, R. A. Rahman, and A. Ahmed, "A study of FBG sensor and electrical strain gauge for strain measurements," *Journal of Optoelectronics and Advanced Materials*, vol. 10, no. 10, pp. 2564-2568, Oct. 2008.
- [8] X. Yang, S. Luo, Z. Chen, J. H. Ng, and C. Lu, "Fiber Bragg grating strain sensor based on fiber laser," *Optics Communications*, vol. 271, no. 1, pp. 203-206, Mar. 2007, doi: 10.1016/j.optcom.2006.10.007.
- [9] C. Vendittozzi, F. Felli, and C. Lupi, "Modeling FBG Sensors Sensitivity from Cryogenic," *Optical Fiber Technology*, vol. 42, pp. 84-91, May 2018, doi: 10.1016/j.yofte.2018.02.017.
- [10] S. Daud, M. A. Jalil, S. Najmee, T. Saktioto, J. Ali, and P. P. Yupapin, "Development of FBG Sensing System for Outdoor temperature environment," *Procedia Engineering*, vol. 8, pp. 386-392, 2010, doi: 10.1016/j.proeng.2011.03.071.
- [11] M. A. I. Jahan, R. V. Honnunar, and R. Versha, "Analysis of FBG Sensor for Accurate Pressure Sensing with Improved Sensitivity," *Materials Today: Proceedings*, vol. 5, no. 2, pp. 5452-5458, 2018, doi: 10.1016/j.matpr.2017.12.133.
- [12] R. Kashyap, "Fiber Bragg Grating," *USA: Academic Press*, 1999.
- [13] A. Issatayeva, A. Beisenova, D. Tosi, and C. Molardi, "Fiber-Optic Based Smart Textiles for Real-Time Monitoring of Breathing Rate," *Sensors*, vol. 20, no. 12, pp. 1-16, Jun. 2020, doi: 10.3390/s20123408.
- [14] L. Dziuda, F. W. Skibniewski, M. Krej, and J. Lewandowski, "Monitoring respiration and cardiac activity using fiber Bragg grating-based sensor," *IEEE Transactions on Biomedical Engineering*, vol. 59, no. 7, pp. 1934-1942, Jul. 2012, doi: 10.1109/TBME.2012.2194145.
- [15] C. Chen, Q. Wu, K. Xiong, H. Zhai, N. Yoshikawa, and R. Wang, "Hybrid Temperature and Stress Monitoring of Woven Fabric Thermoplastic Composite using Fiber Bragg Grating based Sensing Technique," *Sensors*, vol. 20, no. 11, pp. 1-17, May 2020, doi: 10.3390/s20113081.
- [16] S. R. Tahhan, M. H. Ali, M. A. Z. Al-Ogaidi, and A. K. Abass, "Impact of Apodization Profile on Performance of Fiber Bragg Grating Strain-Temperature Sensor," *Journal of Communications*, vol. 14, no. 1, pp. 53-57, Jan. 2019, doi: 10.12720/jcm.14.1.53-57.
- [17] H. M. El-Gammal, E. S. A. El-Badawy, M. R. Rizk, and M. H. Aly, "A New Hybrid FBG with a π -Shift for Temperature Sensing in Overhead High Voltage Transmission Lines," *Optical and Quantum Electronics*, vol. 52, no. 53 pp. 1-24, Jan. 2020, doi: 10.1007/s11082-019-2171-7.
- [18] C. R. U. Kumari, D. Samiappan, R. Kumar, and T. Sudhakar, "Development and Experimental Validation of a Nuttallapodized Fiber Bragg Grating Sensor with A Hydrophobic Polymer Coating Suitable for Monitoring Sea Surface Temperature," *Optical Fiber Technology*, vol. 56, May 2020, doi: 10.1016/j.yofte.2020.102176.
- [19] X. Zhou, Y. Zhou, Z. Li, M. Bi, G. Yang, and T. Wang, "Research on Temperature Sensing Characteristics with Cascaded Fiber Sagnac Interferometer and Fiber Fabry-Perot Interferometer-based Fiber Laser," *Optical Engineering*, vol. 58, no. 5, May 2019, doi: 10.1117/1.OE.58.5.057103.
- [20] D. Irawan, T. Saktioto, J. Ali, and P. Yupapin, "Design of Mach-Zehnder Interferometer and Ring Resonator for Biochemical Sensing," *Photonics Sensor*, vol. 5, no. 1, pp. 12-18, 2015, doi: 10.1007/s13320-014-0200-5.
- [21] Y. Ying, N. Hu, G. Y. Si, K. Xu, N. Liu, and J. Z. Zhao, "Magnetic Field and Temperature Sensor based on D-Shaped Photonic Crystal Fiber," *Optik*, vol. 176, pp. 309-314, Jan. 2019, doi: 10.1016/j.ijleo.2018.09.107.

- [22] R. F. Syahputra, Saktioto, R. Meri, Syamsudhuha, and Okfalisa, "Profile of single mode fiber coupler combining with Bragg grating," *TELKOMNIKA Telecommunication Computing Electronics and Control*, vol. 15, pp. 1103-1107, 2017, doi: 10.12928/TELKOMNIKA.v15i3.6383.
- [23] P. S. Reddy, R. N. S. Prasad, D. Sengupta, M. S. Shankar, and K. Srimannarayana, "Teflon-Coated Fiber Bragg Grating Sensor for Wide Range of Temperature Measurements," *Journal of Optoelectronics and Advanced Materials*, vol. 12, no. 10, pp. 2040-2043, Oct. 2010.
- [24] C. K. Kao, "Nobel Lecture: Sand from Centuries Past: Send Future Voices Fast," *Reviews of Modern Physics*, vol. 82, no. 3, pp. 2299-2303, Aug. 2010, doi: 10.1103/revmodphys.82.2299.
- [25] X. Jin, S. Yuan, and J. Chen, "On Crack Propagation Monitoring by using Reflection Spectra of AFBG and UFBG Sensors," *Sensors and Actuators A: Physical*, vol. 285, pp. 491-500, Jan. 2019, doi: 10.1016/j.sna.2018.11.052.
- [26] C. K. Kao, "Sand from Centuries Past: Send Future Voices Fast," *Physics-Uspekhi*, vol. 53, no. 12, pp. 71-81, 2010.
- [27] J. S. Van Delden, "Optical Circulators Improve Bidirectional Fiber Systems," *Laser Focus World*, vol. 31, pp. 109-112, 1995.
- [28] A. F. Sayed, F. M. Mustafa, A. A. M. Khalaf, and M. H. Aly, "Apodized Chirped Fiber Bragg Grating for Postdispersion Compensation in Wavelength Division Multiplexing Optical Networks," *International Journal of Communication Systems*, pp. 1-13, Jul. 2020, doi: 10.1002/dac.4551.
- [29] Q. Guo *et al.*, "Femtosecond Laser Fabricated Apodized Fiber Bragg Gratings Based on Energy Regulation," *Photonics*, vol. 8, no. 4, pp. 1-9, Apr. 2021, doi: 10.3390/photonics8040110.
- [30] R. Measures, "Structural Monitoring with Fiber Optic Technology," USA: Academic Press, 2001.
- [31] M. G. Xu, J. L. Archambault, L. Reekie, and J. P. Dakin, "Thermally-compensated bending gauge using surfacemounted fiber gratings," *International Journal of Optoelectronics*, vol. 9, no. 3, pp. 281-285, 1994.
- [32] R. B. Blackman and J. W. Tukey, "The Measurement of Power Spectra," New York: Dover Publications, 1985.
- [33] N. A. Mohammed, Mohammed, T. A. Ali, and M. H. Aly, "Performance Optimization of Apodized FBG-based Temperature Sensors in Single and Quasi-Distributed DWDM System with New and Different Apodization Profiles," *AIP Advances*, vol. 3, no. 12, pp. 1-21, 2013, doi: 10.1063/1.4859115.
- [34] I. P. Johnson *et al.*, "Optical Fibre Bragg Grating Recorded in TOPAS Cyclic Olefin Copolymer," *Electronics letters*, vol. 47, no. 4, pp. 271-272, Feb. 2011, doi: 10.1049/el.2010.7347.
- [35] M. Rosenberger, S. Hessler, S. Belle, B. Schmauss, and R. Hellmann, "Fabrication and Characterization of Planar Bragg Gratings in TOPAS Polymer Substrates," *Sensors and Actuators A: Physical*, vol. 221, pp. 148-153, Jan. 2015, doi: 10.1016/j.sna.2014.10.040.

BIOGRAPHIES OF AUTHORS



Toto Saktioto is a Senior lecturer at Physics Dept., Faculty of Mathematics and Natural Sciences, Universitas Riau, Pekanbaru, Indonesia. He works on Plasma and Photonics Physics. He has published many articles and supervised Master and Doctoral degree since 2009. Currently his research focus is phonics and plasma industry for communication and biosensors.



Khaikal Ramadhan was a student at the University of Riau in 2017 and has finished studying Physics at the University of Riau with a B.Sc degree in 2021. His interests include applied physics and pure physics.



Yan Soerbakti is a postgraduate student at the University of Riau in 2021 and has completed his undergraduate course in Physics at the University of Riau with a B.Sc degree in 2020. His works of interest include applied physics and pure physics.



Romi Fadli Syahputra is an alumni student of the Physics Department, University of Riau, who has completed his undergraduate studies with a B.Sc degree in 2016 and postgraduate with an M.Sc degree in 2020. Now he works as a lecturer at the Physics Department of Muhammadiyah Riau University. His works of interest include applied physics and pure physics.



Dedi Irawanis is a lecturer at Physics Education, Dept. of Education of Mathematics and Natural Sciences, Universitas Riau, Pekanbaru, Indonesia. He works on basic and advanced Photonics. He has published many articles and supervised Master degree since 2019.



Okfalisa is a Seniorat Department of Informatics Engineering, UIN Sultan Syarif Kasim Riau. She was obtained doctorate degree from Information System at Universiti Teknologi Malaysia (UTM) in 2011. Her interests are in knowledge management system, knowledge base, expert system and information system.